MEASUREMENT OF ETHYLENE CONCENTRATIONS AT HIGH PRESSURE BASED ON TUNABLE DIODE LASER ABSORPTION SPECTROSCOPY NEAR 1620 nm

T. Zhang, G. Zhang, X. Liu, G. Gao, T. Cai*

College of Physics and Electronic Engineering, Jiangsu Normal University, Xuzhou, China; e-mail: *caitingdong@126.com*

A system for detection of ethylene (C_2H_4) at high pressure is developed based on tunable diode laser absorption spectroscopy using a distributed feedback laser near 1620 nm. To eliminate the influence of spectral line overlap under high pressure, a differential absorption (peak minus valley) scheme is adopted. The peak and valley wavelengths used for the measurement correspond to 6174.64 and 6174.45 cm^{-1}, respectively. Absorption cross sections of ethylene are measured for the selected peak and valley wavelength. The measured concentration agrees with the known concentration, and the maximum of the standard deviation is 0.746% for all measurements. In addition, long-term continuous measurements indicated good stability of the system. The sensitivity of the system is ~18 ppm with an optimum averaging time of 110 s. All the experimental results validate the applicability of the system in ethylene trace detection.

Keywords: *tunable diode laser absorption spectroscopy, differential absorption, ethylene, concentration, high pressure.*

ИЗМЕРЕНИЕ КОНЦЕНТРАЦИИ ЭТИЛЕНА ПРИ ВЫСОКОМ ДАВЛЕНИИ МЕТОДОМ ПЕРЕСТРАИВАЕМОЙ ДИОДНОЙ ЛАЗЕРНОЙ АБСОРБЦИОННОЙ СПЕКТРОСКОПИИ ВБЛИЗИ ДЛИНЫ ВОЛНЫ 1620 нм

T. Zhang, G. Zhang, X. Liu, G. Gao, T. Cai*

УДК 543.42;621.378.8

Колледж физики и электронной инженерии, Педагогический университет Цзянсу, Сюйчжоу, Китай; e-mail: caitingdong@126.com

(Поступила 2 июля 2019)

Разработана система детектирования этилена (C_2H_4) при высоком давлении методом перестраиваемой диодно-лазерной абсорбционной спектроскопии с использованием лазера с распределенной обратной связью вблизи 1620 нм. Для устранения влияния перекрытия спектральных линий при высоком давлении принята дифференциальная схема поглощения (пик минус провал). На выбранных длинах волн пика и провала 6174.64 и 6174.45 $см^{-1}$ определены поперечные сечения поглощения этилена. Измеренная концентрация хорошо согласуется с известной, максимальное стандартное отклонение 0.746%. Длительные непрерывные измерения показывают хорошую стабильность системы. Чувствительность системы ~18 ppm при оптимальном времени усреднения 110 с. Экспериментальные результаты подтверждают применимость данной системы для обнаружения следов этилена.

Ключевые слова: *абсорбционная спектроскопия на перестраиваемых диодных лазерах, дифференциальное поглощение, этилен, концентрация, высокое давление.*

Introduction. Ethylene (C_2H_4) is one of the most important products in chemical raw materials. It is widely used in the production of hydrocarbons and many other intermediate products [1]. Ethylene can also be mixed with air to form explosive mixtures. When exposed to open fire, high heat, or contact with oxidants, there is a risk of fire and explosion [2]. Therefore, it is of great significance to develop an ethylene gas detection technology.

There are various studies on the detection of ethylene. Platz et al. described sub-Doppler overtone spectroscopy of C_2H_4 with optoacoustic and optothermal spectra in the range of 6147–6170 cm^{-1} [3]. Hai Pham-Tuan et al. presented an automated capillary gas chromatographic system to measure ethylene in biological materials [4]. Sgro examined the solubility in water of combustion generated organic particulate matter by comparing the ultraviolet visible spectra (UV-Vis) observed in situ in rich ethylene air flames with the spectra of extra situ sampled material trapped in water [5]. However, these methods all have some disadvantages. For example, the detection cycle of a gas chromatograph is long, which is not suitable for real-time monitoring; the UV-Vis is susceptible to water vapor interference.

In order to solve these problems, the technology of tunable diode laser absorption spectroscopy (TDLAS) based on the Beer-Lambert law was used in this paper, and the gas concentration was obtained by analyzing changes in the selected absorption line [6]. This technique is widely used in trace gas detection due to its advantages of non-invasiveness, high spectral resolution, and high selectivity [7–10]. It has also been used for the detection of C_2H_4. For example, Lucchesini et al. examined absorption lines of C_2H_4 near 12000 cm^{-1} by using a tunable diode laser spectrometer combined with wavelength modulation spectroscopy and a Herriot type multipass cell [11]. Pan et al. developed a TDLAS system for the simultaneous measurement of C_2H_4 and CH_4 at 6150 cm^{-1} and established a line separation method based on multi absorption peak using the least squares algorithm. The accuracy of the measured concentration was within 5% compared with the mass flow meter [12]. Wei et al. proposed a nine optical fiber multi-point ethylene concentration sensor based on TDLAS. By using WMS and a gas cell, a ppm-level high sensitivity detecting system for ethylene concentration was achieved [13]. Tanaka et al. reported a mid-infrared sensor for detecting ethylene in combustion exhaust [14]. In our previous work [15], we used photoacoustic spectroscopy to measure low-concentration C_2H_4 by using the transition in the near-infrared region with the detection of the second harmonic signal of the absorption spectrum. All these works are performed at normal pressure or low pressure. According to our investigation, there are relatively few studies that measured C_2H_4 at high pressure.

It is known that only the absorption lines of ethylene in the range of 3–14 μm were recorded in the HITRAN database [16]. Here we measure some of its transitions in the near-infrared band. The measured and simulated C_2H_4 absorption spectra near 6175 and 3032 cm^{-1} at room temperature are shown in Fig. 1a,b, respectively. The simulated H_2O, CO_2, and CH_4 absorption spectra in the responding regions are also given in the figure. It can be seen from the figure that the C_2H_4 absorbance near 3032 cm^{-1} is merely 30 times stronger than the absorbance near 6175 cm^{-1}, but lasers, detectors, and optical elements near 3032 cm^{-1} are more expensive than those near 6175 cm^{-1}. It can be seen from the figure that the interference of CO_2 and CH_4 on ethylene is negligible in both regions, but C_2H_4 transitions in this mid-infrared region overlap with some strong transitions of H_2O. Hence the C_2H_4 transitions near 6175 cm^{-1} is more suitable for the development of the system for C_2H_4 detection. However, it must be noted that C_2H_4 transitions near 6175 cm^{-1} are also dense. The overlap of these lines will be serious at high pressure, and an isolated line cannot be observed at high pressure. In order to detect C_2H_4 at high pressure, here a system based on TDLAS and a differential absorption (peak-minus-valley) scheme will be built and illustrated in a static cell with high pressure.

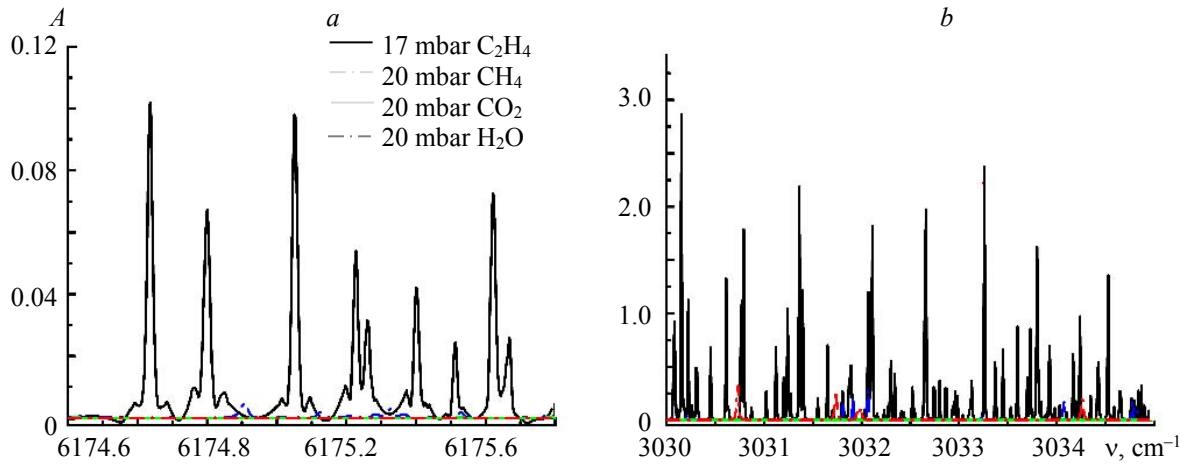

Fig. 1. Example of the ethylene absorption spectrum in the near- and mid-infrared region.

Experiment and scheme. A schematic diagram of the experimental configuration is depicted in Fig. 2a. The light source is a continuous-wavelength (CW) distributed-feedback (DFB) tunable diode laser (Diantuo Laser Technology, BF14-DFB-1620) emitting radiation near 1620 nm with a typical linewidth of ~2 MHz. The laser is driven by a commercial laser controller (Thorlabs, CLD101x). The diode laser output performance is shown in Fig. 2b. The experimentally determined current tuning coefficients of the laser are ~0.025 cm^{-1}/mA. The maximum optical power emitted by the diode laser operating at a temperature of 13.8°C and an injection current of 100 mA is ~11 mW. During the experiment, the laser temperature is fixed and its current is driven by a 100 Hz triangle ramp provided by a function generator (RIGOL, DG1000Z) for the wavelength. The laser beam is divided by a splitter into two parts: one is sent into a wavelength meter (Bristol Instrument, 671B), whose wavelength accuracy is as high as ±0.0008 nm to confirm the center wavelength of the laser before the measurement, and the other part is injected into the gas cell. The cell has a path length of 50 cm and a volume of 0.3 L. The beam is passed through the gas cell and focused on a photoelectric detector. The signal obtained from the photoelectric detector is sampled by a data acquisition device (16 bits, 2 MS/s) at a maximum sample rate of 10 KS/s. A LABVIEW based program with two channels is used to record the measured signal and the triangle wave.

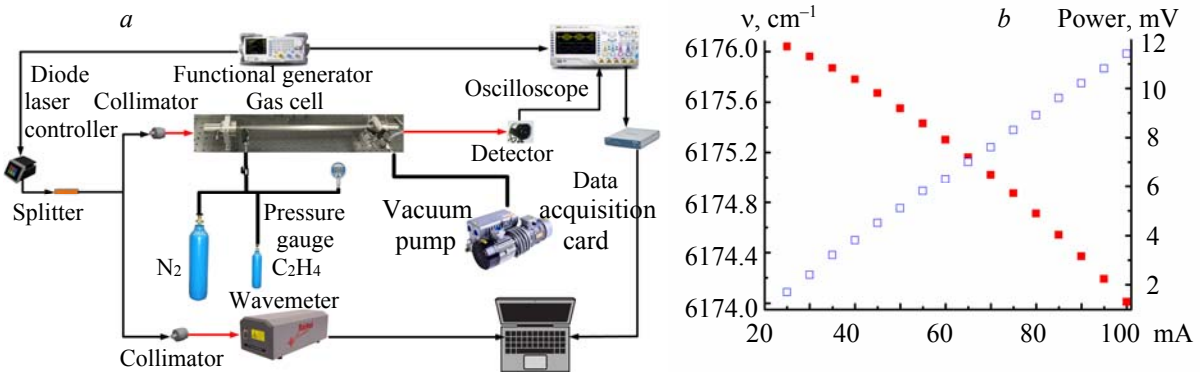

Fig. 2. a) Schematic of the high-pressure experimental setup. b) Output performance of the CW-DFB diode laser as a function of injection current at an operating temperature of ~13.8°C.

Before each measurement, the gas cell is evacuated to less than –100 kPa using a rotary-vane vacuum pump with a standard speed of 1400 r/min, and then the background I_0 signal is obtained by filling the cell with N_2 gas at the measurement pressure. The stainless steel, tube is filled with a known proportion of N_2-diluted ethylene. When the gas is completely mixed for a period of time, the mixed gas is delivered into the gas cell. The pressure inside the cell and tube is indicated by a pressure gauge with an accuracy of ±1% of reading.

The differential absorption (peak minus valley) scheme is based on the direct absorption theory and gives the concentration of trace gases according to the intensity of narrow band absorption. Since the bandwidth interference remains constant on the selected absorption transition, the interference can be eliminated by the difference between the peak and valley of the absorption line. In addition, the scheme eliminates the problems of laser intensity loss due to scattering and extinction.

According to the Beer–Lambert law, when a laser beam passes through a gas cell filled with an absorbed gas, the transmitted intensity $I(\nu)$ in the frequency ν is determined by

$$\ln\left(I(\nu)/I_0\right) = \frac{\sigma(\nu,T,P)P_iL}{RT} = \alpha(\nu,T,P), \quad (1)$$

where I_0 is the incident intensity before absorption, ν is the frequency in cm^{-1}; T is the temperature in K; P_i is the partial pressure of the absorbing species in atm; R (8.314 J/K·mol) is the universal gas constant; L is the laser pathlength in meters; $\alpha(\nu, T, P)$ is the absorbance, and $\sigma(\nu, T, P)$ is the absorption cross-section in cm^2/molecule, which depends on the wavelength, temperature, and pressure. If T, P_i, L, $\alpha(\nu, T, P)$, and $\sigma(\nu, T, P)$ are known, we can calculate the mole fraction of C_2H_4.

In the absolute condition, the attenuation of light intensity caused by absorption in the atmosphere can be expressed by Eq. (1). However, interference factors such as Rayleigh scattering and Mie scattering caused by fume, droplets, or aerosol cannot be ignored. So, when considering these influences, the above equation

can then be written as

$$\ln(I/I_0) = \alpha_{C_2H_4} + \alpha_{int} + \tau_{ext}, \quad (2)$$

where $\alpha_{C_2H_4}$ is the absorption of the ethylene, α_{int} is the total interference absorption from all other species, and τ_{ext} includes the effect of total extinction (absorption and scattering) from all other sources.

As evidenced above, in order to measure the ethylene concentration, it is necessary to eliminate the interference and extinction from other components in the selected band. The transmitted loss caused by interference and extinction is wavelength dependent. However, these losses are almost constant over a small wavelength shift, and thus the differential absorption strategy can adequately eliminate the effect of these non-absorption laser losses of the laser. In this differential scheme, the interference and extinction can be eliminated by using the difference between the absorption at selected peak and valley wavelength:

$$\ln(I/I_0)_{\nu,peak} - \left(-\ln(I/I_0)_{\nu,valley}\right) = \left(\alpha_{C_2H_4} + \alpha_{int} + \tau_{ext}\right)_{\nu,peak} - \left(\alpha_{C_2H_4} + \alpha_{int} + \tau_{ext}\right)_{\nu,valley} \approx \alpha_{C_2H_4(\nu,peak)} - \alpha_{C_2H_4(\nu,valley)}. \quad (3)$$

Therefore, the ethylene mole fraction can be obtained when the cross sections at the peak and valley are known:

$$\chi_{C_2H_4} = \frac{-\ln\left(\left(I_{(\nu,peak)} / I_{0(\nu,peak)}\right)\left(I_{0(\nu,valley)} / I_{(\nu,valley)}\right)\right)}{\left(\sigma_{(\nu,peak)} - \sigma_{(\nu,peak)}\right) P_{total} L / RT}. \quad (4)$$

Results and discussion. In order to select the peak and valley position within the spectral range of interest, the experimental spectra are measured under different pressures. An overview of the recorded spectra of C_2H_4 at different pressures between 6174.2 and 6175.6 cm^{-1} is presented in Fig. 3.

The wavelength selection criteria for measuring the concentration of species have been reported in [17]. Because the line width is proportional to the total pressure, the shape of each line will be broadened and the spectra will merge. It can be seen from Fig. 3 that no isolated line can be observed in the selected region at a pressure of 3 atm. Taking into account the pressure-induced broadening, the wavelength with the maximum differential absorption cross section and the wavelength with the minimum peak-to-trough spacing, as well as the small pressure shift, the peak and valley located at 6174.64 and 6174.45 cm^{-1} are selected for the experiment, as shown in Fig. 3.

In order to deduce the concentration of ethylene using the differential absorption (peak minus valley) scheme, the absorption cross sections of ethylene at the peak and valley wavelengths selected in the experiment are measured. The ethylene absorption cross sections are measured with C_2H_4/N_2 mixtures of different concentrations. All measurements are performed over a range of pressure (1–6 atm) at a temperature of 303 K. As an example, the absorbance measured at the peak and valley is plotted as a function of mole fraction under 2 atm in Fig. 4. It can be seen from the figure that a linear relationship holds; the correlations of these measured points have R^2 values of 0.999 and 0.998, respectively.

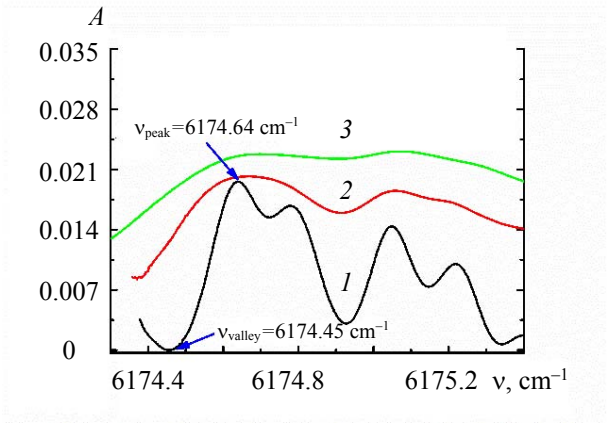

Fig. 3. Diagram of the measured TDLAS spectrum of C_2H_4 between 6174.2 and 6175.6 cm^{-1} at different pressures; P = 1 atm, $X_{C_2H_4}$=5.00% (1), P = 2 atm, $X_{C_2H_4}$=5.03% (2), P = 3 atm, $X_{C_2H_4}$= = 5.04% (3); T = 303 K.

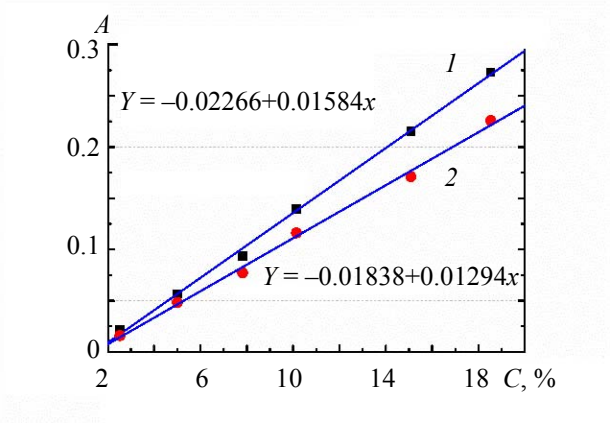

Fig. 4. Relationship between the C_2H_4 concentration and absorbance measured at the peak (1) and valley (2); P = 2 atm; T = 303 K.

TABLE 1. Absorption Cross Sections at the Peak and Valley Wavelengths Selected in the Experiment at Different Pressures

P, atm	σ_{peak}, m^2/mol	σ_{valley}, m^2/mol
1	1.117	0.795
2	0.916	0.781
3	0.859	0.764
4	0.802	0.755
5	0.785	0.750
6	0.770	0.735

The absorption cross section $\sigma(\nu, T, P)$ describes the capacity of a specific gas molecule itself to absorb the amount of light intensity; its value is determined by the gas absorption wavelength, the gas temperature, and the total pressure. The good linear relationship of the data in Fig. 4 indicates a high accuracy of the absorption cross section obtained from the measured ethylene absorption line. However, the deviation of the standard gas purity, the experimental environment, and the gas concentration ratio will introduce errors in the absorption cross section measurements. Table 1 shows measured values of the absorption cross sections at the peak and valley wavelength selected in the experiment at different pressures. It shows that the absorption cross-section decreases gradually as the pressure increases.

The spectral absorbance can be determined from the ethylene absorption signal and the background signal according to the Beer–Lambert law. Then the concentration of C_2H_4 can be calculated using Eq. (4) with the known temperature, pressure, gas cell length, and absorption cross section. Experiments were performed in the pressure range of 1–6 atm with a step of 1 atm. The C_2H_4 concentrations obtained by the differential absorption scheme at various pressures are compared with the known concentrations in Fig. 5. The maximum of the standard deviation between the measured and known C_2H_4 concentrations is 0.746% over the entire pressure range. Those results confirm the accuracy of the system for the measurement of C_2H_4 concentration at high pressure.

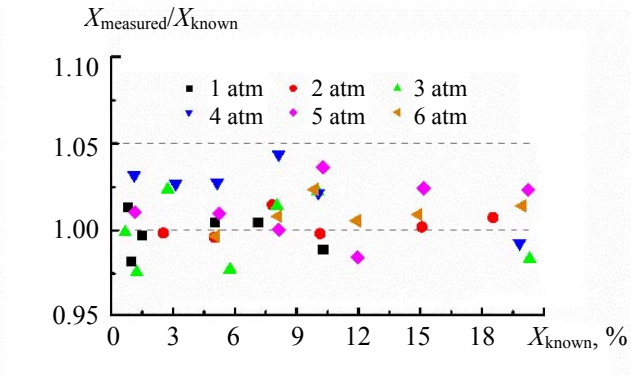

Fig. 5. Comparison of C_2H_4 concentrations measured by the differential absorption scheme with known concentrations at different pressure.

Stability and precision are important parameters for evaluating the performance of a system for spectral measurements [18]. In fact, the stability of the system will be affected by changes in the environment and instrument temperatures, drifts in laser intensity and frequency, variations in the interference fringes, and background noise. In order to evaluate the measurement accuracy and stability of the high-pressure C_2H_4 concentration detection system, time series measurements of C_2H_4-N_2 sealed in the static cell (having a constant concentration) are performed. Each measurement is performed by averaging 30 scans with a scan rate of 100 Hz. One thousand data points are obtained during one-hour of continuous measurement. A histogram of the measured concentrations depicting an approximate normal distribution around the mean value is plotted in Fig. 6a, which can be used to assess the measurement precision. A Gaussian profile is fitted to the distribution histogram, resulting in a half-width at half-maximum (HWHM) of 10.4 ppm.

The Allan variance is usually used to evaluate the noise components of the system [19, 20]. Thus, the sensitivity of the C_2H_4 measurement at high pressure based on the differential absorption scheme is determined by the Allan analysis in the experiment. The sample gas is a C_2H_4-N_2 mixture with 0.5% C_2H_4

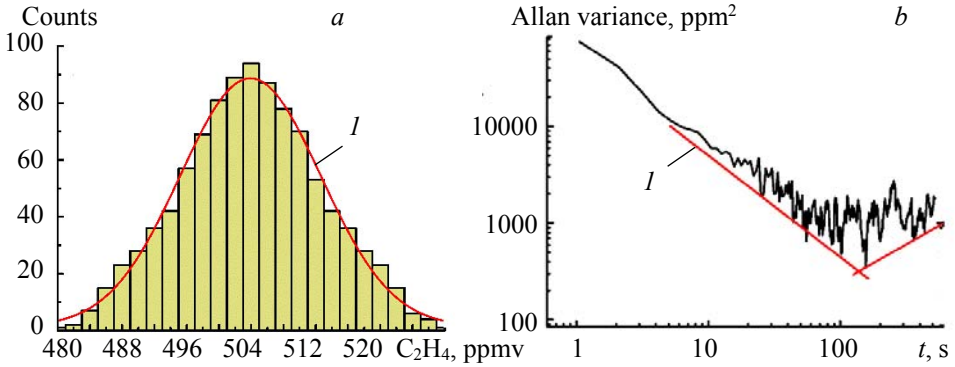

Fig. 6. a) Histogram plot obtained from time series measurements of C_2H_4 sealed in the static cell; the line 1 depicts a Gaussian profile. b) Allan deviation from the time series measurements for the same mixture.

at a pressure of ~3 atm. Figure 6b shows the Allan variance obtained from the continuous time series measurements for the sample gas. It can be seen from the figure that the sensitivity of the system is ~18 ppm with an optimum averaging time of 110 s.

Acknowledgements. The work is funded by the National Natural Science Foundation of China (NSFC) (61875079, 61805110, 61475068, 11104237) and the Science and Technology Program of Xuzhou City (No. KC19202).

REFERENCES

1. Ilias K. Nikolaidis, Luis F. M. Franco, Luc N. Vechot, Ioannis G. Economou, *Fluid Phase Equilibr.*, **470**, 149–163 (2018).
2. Bo Gan, Be Li, Haipeng Jiang, Dawei Zhang, Mingshu Bi, Wei Gao, *J. Loss Prevent. Proc. Ind.*, **54**, 93–102 (2018).
3. P. Platz, W. Demtr Öder, *Chem. Phys. Lett.*, **294**, N 4-5, 397–405 (1998).
4. Hai Pham-Tuan, Joeri Vercammen, Christophe Devos, Pat Sandra, *J. Chromatogr. A*, **868** (2000).
5. L. A. Sgro, P. Minutolo, G. Basile, A. D'Alessio, *Chemosphere*, **42**, 671–680 (2001).
6. Jingsong Li, Benli Yu, Weixiong Zhao, Weidong Chen, *Appl. Spectrosc. Rev.*, **49**, N 8, 666–691 (2014).
7. Andreas Hangauer, Armin Spitznas, Jia Chen, Rainer Strzoda, Hans Link, Maximilian Fleischer, *Proc. Chem.*, **1**, N 1, 955–958 (2009).
8. Chunguang Li, Lei Dong, Chuantao Zheng, Frank K. Tittel, *Sens. Actuat. B: Chem.*, **232**, 188–194 (2016).
9. R. Ghorbani, F. M. Schmidt, *Opt. Express*, **25**, N 11, 12743–12752 (2017).
10. Chuantao Zheng, Weilin Ye, Nancy P. Sanchez, Chunguang Li, Lei Dong, Yiding Wang, Robert J. Griffin, Frank K. Tittel, *Sens. Actuat. B: Chem.*, **244**, 365–372 (2017).
11. A. Lucchesini, S. Gozzini, *J. Quant. Spectrosc. Radiat. Transf.*, **112**, N 9, 1438–1442 (2011).
12. Wei Dong Pan, Jia Wei Zhang, Jing Min Dai, Yu Feng Zhang, *J. Infrared Millimeter Waves*, **32**, N 6, 486–790 (2013).
13. Yubin Wei, Jun Chang, Jie Lian, Tongyu Liu, *Photon. Sens.*, **5**, N 1, 67–71 (2015).
14. Kotaro Tanaka, Kazushi Akishima, Masahiro Sekita, Kenichi Tonokura, Mitsuru Konno, *Appl. Phys. B*, **123**, N 8 (2017).
15. Ch. Ying, G. Guangzhen, C. Tingdong, *Chin. J. Lasers*, **44**, N 5 (2017).
16. L. S. Rothman, I. E. Gordon, Y. Babikov, A. Barbe, D. Chris Benner, P. F. Bernath, M. Birk, L. Bizzocchi, V. Boudon, L. R. Brown, A. Campargue, K. Chance, E. A. Cohen, L. H. Coudert, V. M. Devi, B. J. Drouin, A. Fayt, J.-M. Flaud, R. R. Gamache, J. J. Harrison, J.-M. Hartmann, C. Hill, J. T. Hodges, D. Jacquemart, A. Jolly, J. Lamouroux, R. J. Le Roy, G. Li, D. A. Long, O. M. Lyulin, C. J. Mackie, S. T. Massie, S. Mikhailenko, H. S. P. Müller, O. V. Naumenko, A. V. Nikitin, J. Orphal, V. Perevalov, A. Perrin, E. R. Polovtseva, C. Richard, M. A. H. Smith, E. Starikova, K. Sung, S. Tashkun, J. Tennyson, G. C. Toon, Vl .G. Tyuterev, G. Wagner, *J. Quant. Spectrosc. Radiat. Transf.*, **130**, 4–50 (2013).
17. S. H. Pyun, J. Cho, D. F. Davidson, R. K. Hanson, *Meas. Sci. Technol.*, **22**, N 2, 025303 (2011).
18. T. J. A. Butler, J. L. Miller, A. J. Orr-Ewing, *J. Chem. Phys.*, **126**, N 17 (2007).
19. D. W. Allan, J. A. Barnes, *35th Frequency Control Symp.*, **36**, N 5, 470–475 (1981).
20. D. W. Allan, *Proc. IEEE*, **54**, N 2, 221–230 (1966).